Available online at www.sciencedirect.com

ScienceDirect

Energy Procedia 114 (2017) 4411 – 4423

Energy Procedia

13th International Conference on Greenhouse Gas Control Technologies, GHGT-13, 14-18 November 2016, Lausanne, Switzerland

CO_2 storage: setting a simple bound on potential leakage through the overburden in the North Sea Basin

R.A. Chadwick[a], G.A. Williams[b], D.J. Noy[a]*

[a]*British Geological Survey, Environmental Science Centre, Keyworth, Nottinghamshire, UK. NG12 5GG*

Abstract

So-called 'gas chimneys' are likely to provide the main geological risk for out-of-reservoir CO_2 migration in thick post-rift overburden successions such as typify the central and northern North Sea. Here we postulate that, in the North Sea, such chimneys formed in the geological past, with a likely peak activity at the end of the ice-age, and are currently rather dormant. With this postulate we set a bound on possible bulk migration rates considering both advective and diffusive flow and based on a hypothetical CO_2 storage site at 800 m depth. Calculated migration velocities into the overburden, by either advection or diffusion, are very low, at less than one metre per thousand years. Consequently flux rates are also very low, several orders of magnitude below the leakage thresholds that have been suggested as ensuring effective mitigation performance. Time-lapse seismic reflection data from the Sleipner storage site, which is located beneath some small chimney features, show no evidence of CO_2 migration into the overburden. This cannot prove the postulate, because the time interval spanned by the seismic surveys is just a few years, but it is nevertheless consistent with it.

Peer-review under responsibility of the organizing committee of GHGT-13.

Keywords: CCS; CO_2 storage; Sleipner; overburden; leakage.

* Corresponding author. Tel.: +44-(0)115-9363183.
E-mail address: rach@bgs.ac.uk

Peer-review under responsibility of the organizing committee of GHGT-13.
doi:10.1016/j.egypro.2017.03.1597

1. Introduction

The world's main large-scale CO_2 storage opportunities are situated in very thick sedimentary sequences developed on passive continental margins. These commonly contain major hydrocarbon provinces and are typified by the North Sea Basin on the NW European shelf and major modern delta/fan complexes such as are found for example in the Gulf of Mexico, offshore of Brazil and offshore SE Asia.

Potential storage sites in these settings generally have thick overburdens of low permeability sealing strata intercalated with higher permeability reservoir units. Large-scale overburden heterogeneities offer the means to breach sealing sequences by allowing fluids to flow vertically across stratal boundaries. These 'seal by-pass' features are of three main types: geological faults, 'chimneys or pipes' and injected bodies of sedimentary or igneous material [1]. A key issue for CCS is to assess whether the allowable bulk flux through a particular seal by-pass feature would be sufficient to compromise the integrity and efficacy of the storage site over time.

In these settings the greater part of most storage site overburdens lie within the 'post-rift' parts of the sedimentary succession. Post-rift sequences are characterised by a paucity of large throughgoing faults, so chimneys are likely to provide the main risk for by-passing the geological seals. Seismic reflection data provide the key evidence for the existence of chimneys which are characteristically imaged as narrow vertical or sub-vertical zones of disrupted stratal reflections, with strong spatial variation in reflectivity (Fig. 1).

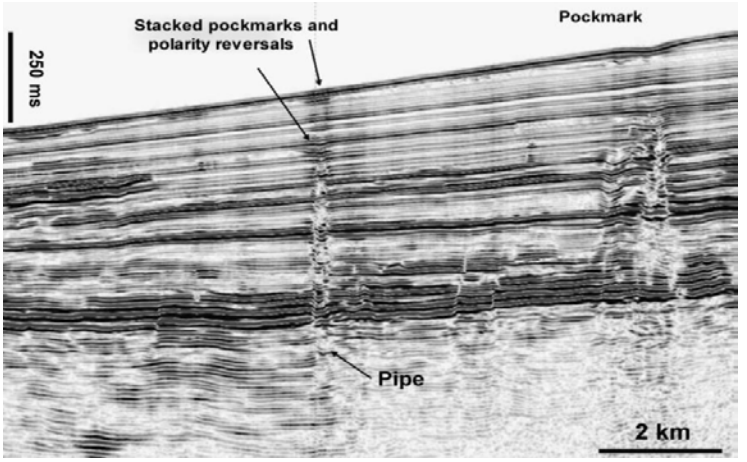

Fig. 1 Small chimneys / pipes imaged on a seismic profile [1]. Reprinted courtesy of the AAPG whose permission is required for further use.

Chimneys are typically a few tens to hundreds of metres in diameter, but can be well in excess of a kilometre in height, allowing them to straddle thick overburden successions. In some cases the seismically-imaged features are linked to overlying pockmarks at the seabed, indicative of significant contemporary fluid flux and high transient permeability and they are believed to have formed conduits for large-scale gas or fluid migration at some point in their history. There is no record in the public domain of any chimney having been sampled in situ, but rare field exposures of exhumed examples suggest that they comprise pipe-like structures with disturbed strata and complex anastomosing fracture networks [2].

1.1. North Sea chimneys

In the North Sea the post-rift sequence ranges up to 3000 m thick and is likely to contain a major proportion of the UK CO_2 storage potential. Chimneys occur commonly throughout the shallower overburden [3]. It is believed that they were initiated as fluid leak-off points from overpressured sedimentary sequences, or during episodes of

rapid pressure decrease leading to in situ expansion of naturally-occurring gas accumulations. The latter would accompany removal of an overlying load such as by rapid tectonic uplift and erosion or melting of an overlying ice-sheet. The thickness of Pleistocene ice cover over the central North Sea is uncertain, but modelling suggests maximum thicknesses in the range 1500 m to 2000 m [4, 5] for the last glacial event and there is evidence that major gas chimney activity in the Barents Sea accompanied melting of the last ice-sheets (Stefan Bunz pers. comm).

An important corollary of this is that North Sea chimneys at the present-day, more than 10000 years after the ice-sheet melting, are perceived to be rather dormant and not currently at their peak of fluid flow. This is supported by the observations that few of them are associated with active pockmarks (Owain Tucker pers. comm.) and natural seabed emissions of deep-sourced gas in the North Sea are low.

This paper aims to set some bounds on CO_2 migration in chimneys by establishing a simple boundary condition on possible chimney properties. We will use a scenario based broadly on the Sleipner storage operation, where some relevant physical properties have been measured, but that is also applicable to storage in other shallow aquifers, or to storage in deeper reservoirs which have overlying 'secondary' storage units.

1.2. Sleipner and its overburden

The Sleipner CO_2 storage project is situated in the Norwegian North Sea (Fig. 2), close to the median line with the UK [6]. Injection commenced in 1996, with at the time of writing around 16 million tonnes of CO_2 stored. The storage reservoir is the Utsira Sand, a regional saline aquifer lying within the upper part of the late Mesozoic-Cenozoic post-rift succession of the North Sea Basin [7, 8]. Time-lapse 3D seismic monitoring surveys were acquired in 1994 (pre-injection baseline), 1999, 2001, 2002, 2004, 2006, 2008 and 2010. These show the injected CO_2 to be trapped at a number of levels within the reservoir, forming a multi-tier seismically reflective plume (Fig. 3a) [9]. The top of the CO_2 plume, trapped beneath the reservoir topseal at a depth of around 800 m, is overlain by about 720 m of overburden strata and 80 m of seawater. Prior to injection, reservoir pressures in the Utsira Sand were hydrostatic (SACS project unpublished data), with only a very small pressure increase observed during injection [10].

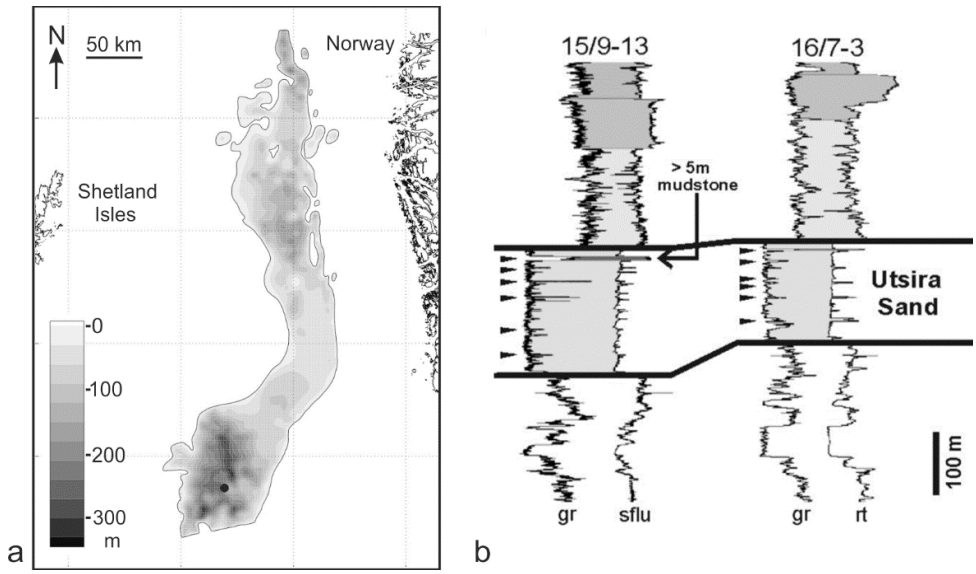

Fig. 2 a) Isopach map of the Utsira Sand with location of Sleipner (black spot) b) Representative geophysical well logs showing the contrast between the reservoir sand with low γ-ray and resistivity readings and the argillaceous overburden with much higher readings (γ-ray logs on the left tracks and resistivity logs on the right tracks).

Wireline logs and well cuttings show the overburden to comprise dominantly mudstones, siltstones with, mostly at shallower depths, occasional sandier beds. The deepest unit of the overburden is the Nordland Shale which forms the reservoir topseal. A core was taken in the lower part of the Nordland Shale in 2002. Laboratory measurements [11, 12] indicate satisfactory sealing capacity, with a permeability of around 4 x 10^{19} m^2 and capillary entry pressures of 3 MPa (to N_2) and 2 - 4 MPa (to CO_2). These values comfortably exceed buoyancy or injection pressures associated with the current CO_2 plume at Sleipner.

The permeability and capillary entry pressures of the core samples indicate therefore, that in an intact water-saturated state, the Nordland Shale acts an effective capillary seal. Cuttings samples and wireline logs from wells in the vicinity, plus observed lateral stratal continuity on seismic data, indicate that the coring point is representative of the wider Utsira topseal and that its properties can be taken as representative of intact caprock more widely.

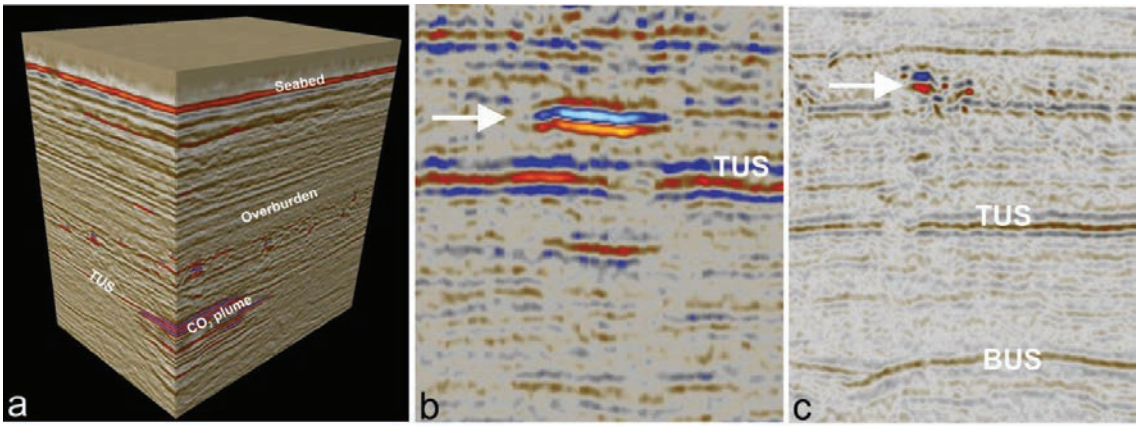

Fig. 3 a) Time-lapse 3D seismic cube in 2006 showing the reflective Sleipner plume b) and c) seismic sections from the baseline 3D dataset (1994) showing two bright-spots (arrowed) in the overburden above the Utsira Sand reservoir. Both are underlain by disturbed and attenuated seismic reflections perhaps indicative of small feeder pathways or chimneys. TUS = Top Utsira Sand, BUS = Base Utsira Sand.

Although there are no major seismic chimneys in the Sleipner area, seismic data do show the overburden to contain numerous 'bright-spots' – high amplitude reflections corresponding to negative acoustic impedance contrasts – which are interpreted as accumulations of natural gas (Fig. 3). The bright-spots were visible on the baseline seismic survey acquired prior to CO_2 injection in 1994 and have remained substantially unchanged since. They are indicative of natural gas migration and trapping on geological time-scales at various levels within the overburden. Some of the bright-spots lie closely above the reservoir top and are underlain by disturbed or attenuated seismic reflections, presumably indicative of small gas chimneys or conduits which appear to sit directly upon the Utsira Sand (Fig. 3).

2. Simplified chimney models

In order to model CO_2 bulk migration in chimneys it is necessary to make some reasonable but simplifying assumptions about their current in situ flow properties. These are extremely poorly-understood. There is little value in assessing fluxes through fluid flow models with arbitrarily assigned flow parameters as these will simply produce results in line with whatever properties are assumed: the 'garbage in - garbage out' scenario. Here we propose a conceptual model for a chimney in dominantly argillaceous lithologies whose bulk permeability depends on two simple controlling parameters: the intrinsic permeability of its internal fracture networks, likely to be a function of the fluid pressure (effective stress), and capillary flow effects within the fractures and pore-space, likely to be a function of the resident fluid phases. The model therefore has four end-members depending on the excess pressure within the chimney and the fluid phases within its pores (Fig. 4).

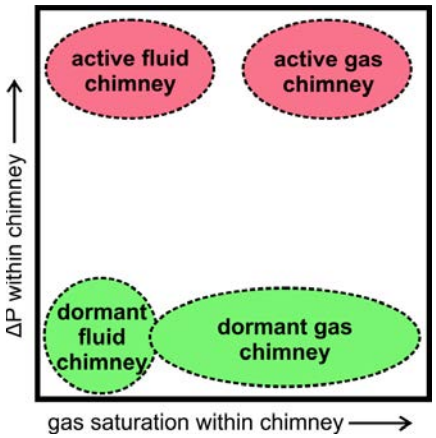

Fig. 4 Conceptual model for chimneys in argillaceous strata

Active chimneys are defined as having significantly elevated pore pressures, with fracture networks in a state of incipient shear or dilation and, as a result, with high effective permeabilities. Dormant chimneys are defined as having pore pressures close to hydrostatic with fracture networks essentially closed and with much lower effective permeabilities, similar to intact rock. The chimney pore-spaces will contain varying proportions of brine and natural gas; we define gas chimneys as containing predominantly natural gas, and fluid chimneys as containing predominantly brine.

2.1. The dormant gas chimney

Our analysis is focussed on dormant chimneys on the hypothesis that these are the current dominant type in the North Sea. As defined, the dormant fluid chimney would have the same effective flow properties as intact overburden and so is not considered further. The dormant gas chimney is more interesting as it is compatible with the observed small chimney features at Sleipner that sit upon the Utsira Sand - they have clearly transmitted natural gas in the past but are likely currently to be at hydrostatic pressure. The component of trapped residual gas will have the effect of lowering the capillary entry pressure to CO_2, reducing the overall sealing capacity of the topseal. Here we set the capillary entry pressure to zero (Fig. 5), which in terms of estimating unwanted CO_2 migration is conservative.

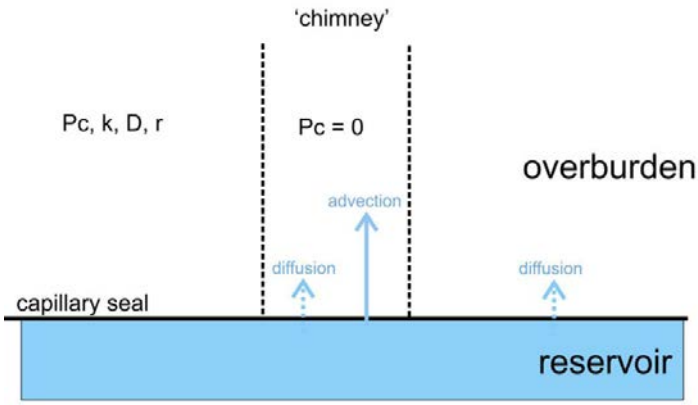

Fig. 5 Schematic of the conceptual dormant gas chimney

3. TOUGH2 flow modelling

When CO_2, either in a dense or gaseous phase, ponds beneath a sealing layer, the driving force for upward migration is provided by its buoyancy plus any reservoir (injection) overpressure. Here we use TOUGH2 modelling of the dormant gas chimney scenario to explore the rate at which this migration might take place and to compare it with migration by diffusion in the aqueous phase. The validity and consequences of assuming Darcy flow within these argillaceous very low permeability strata is discussed later.

The TOUGH2/ ECO2N flow simulator [13, 14] is used for the modelling which is carried out in 1D. The model is based on conditions at the top of the Sleipner storage reservoir, with an overburden thickness of 800 m, hydrostatic reservoir fluid pressures, a temperature gradient of around 32 °Ckm^{-1} [15] and an initial temperature at the top of the reservoir sand of 29 °C. The ECO2N module does not simulate the dense to gaseous phase transition for CO_2, so all model runs were terminated before the advected (free) CO_2 migrated to the depths shallow enough for this to occur. Key model properties (Table 1) are taken from the measured values at Sleipner [11, 12] or more general literature. Values of free CO_2 saturation, dissolved CO_2 concentration and pore pressure in the underlying Utsira Sand are taken from 2D axisymmetric flow models of the CO_2 plume [16].

Table 1. Key TOUGH2 model parameters for the chimney migration scenarios

	Near hydrostatic scenario	Overpressure scenario
Chimney permeability (m^2)	4 x 10^{-19}	4 x 10^{-19}
Chimney porosity (-)	0.3	0.3
Chimney capillary entry pressure (MPa)	0	0
Chimney diffusion co-efficient (m^{2}s^{-1})	5 x 10^{-10}	5 x 10^{-10}
Overpressure at chimney base (MPa)	0.02	2.8

In the following section we explore the overburden migration consequences of two hypothetical 'end-member' pressure scenarios for the dormant gas chimney: one where pressure in the underlying reservoir is assumed to be close to hydrostatic and one where it is just below the fracture limit.

3.1. Near-hydrostatic pressure scenario

This low pressure end-member (Fig. 6) corresponds essentially to the current Sleipner case where overpressure at the base of the chimney is very low [10], and to all intents and purposes limited to buoyancy forces at the plume top.

It is clear that with the very low overpressure, advection into the low permeability seal is extremely slow. The leading-edge of the free CO_2 front advances just 64 m into the overburden in 3 million years (My), with an average migration velocity of ~0.02 m per thousand years (Fig. 6a). The total flux can be obtained by multiplying the migration velocity by the spatial area of the conduit. The actual lateral dimensions of the small overburden chimneys at Sleipner are difficult to determine accurately due to the acoustic shadowing effects of associated shallow gas accumulations (seismic bright-spots), but might be up to 100 m or so in radius. The induced CO_2 chimney within the Sleipner plume itself can be quite accurately measured however [17] with a radius of around 50 m. Taking a notional spatial footprint of 20000 m^2 (corresponding to a notional chimney radius of about 80 m) gives a total amount of advected free CO_2 in the overburden of ~107500 tonnes after 3 My, corresponding to an average flux of ~ 35 tonnes per 1000 years. Upward migration of CO_2 in the aqueous phase, driven by diffusion, is significantly quicker than via advective migration (Fig. 6b). So the first molecules of CO_2 would actually be reaching the seabed in around 3 My. However because concentrations of CO_2 in the aqueous phase are quite small (reducing to zero at the leading edge), the total dissolved CO_2 in the overburden is only ~70500 tonnes after 3 My. This corresponds to a diffusive flux into the overburden of < 25 tonnes of dissolved CO_2 per 1000 years. For this very low advection scenario therefore dissolved CO_2 comprises some 40% of the total CO_2 in the overburden.

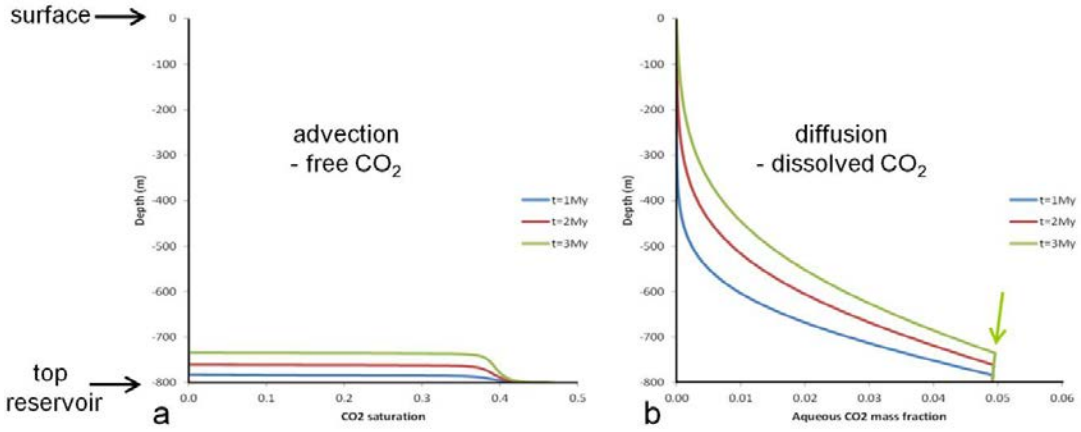

Fig. 6 Near-hydrostatic pressure scenario. 1D TOUGH2 flow simulation of a 'dormant gas chimney', situated on top of a CO_2 plume at 800 m depth. The plots show a) upward migration of buoyant free CO_2 and b) CO_2 diffusing in the aqueous phase. The arrow indicates dissolved CO_2 in fully saturated pore-water behind the advancing free CO_2 front.

3.2. Overpressure scenario

The previous model considered migration driven essentially just by buoyancy forces associated with the free CO_2 plume. In practice, many aquifer storage situations are likely to involve a significant increase in reservoir pore-pressure associated with injection-related water displacement. In this high pressure end-member scenario, CO_2 beneath the topseal is pressurised to just below the fracture limit of the formation.

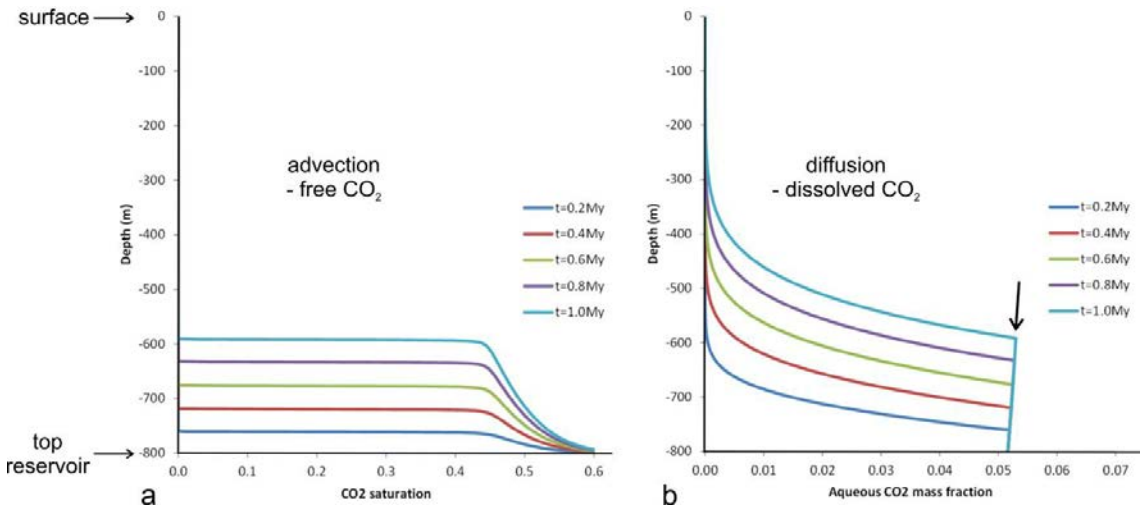

Fig. 7 Overpressure scenario. 1D TOUGH2 flow simulation of a 'dormant gas chimney', situated on top of a CO_2 plume at 800 m depth. The plots show a) upward migration of buoyant free CO_2 and b) CO_2 diffusing in the aqueous phase. The arrow indicates dissolved CO_2 in fully saturated pore-water behind the advancing free CO_2 front.

Leak-off well-test (LOT) data from the North Sea [18] indicate that the onset of fracturing is around 80 – 85 % of lithostatic pressure. In order to remain below this threshold we set a pressure of 10.9 MPa for the CO_2 at the base of the chimney, around 75% of the lithostatic pressure and some 2.8 MPa above hydrostatic. In terms of estimating unwanted CO_2 migration into the overburden this is again conservative because a regulated storage site would probably not allow pressures to rise so close to the fracture threshold. A key aspect of this scenario is that the reservoir pressures, albeit higher than before, still remain below the threshold that the chimney fracture network would come under dilation or shear reactivation. In other words the permeability of the chimney is unchanged from the near-hydrostatic scenario.

With around 2.8 MPa of injection pressure drive, the leading-edge of the free CO_2 front advances about 210 m into the overburden in 1 million years, with an average migration velocity of ~0.2 m per thousand years (Fig. 7a). Advective advance into the overburden is therefore around ten times quicker than by buoyancy alone (Fig. 6a), but still very slow. Taking, as above, the spatial footprint of a typical small CO_2 chimney at Sleipner as 20000 m^2 gives a total amount of advected free CO_2 in the overburden of ~441000 tonnes after 1 My, corresponding to an average flux of ~ 440 tonnes per 1000 years. Upward migration of CO_2 in the aqueous phase results in a total dissolved CO_2 in the overburden of ~60500 tonnes after 1 My. This corresponds to a diffusive flux into the overburden of ~60 tonnes of dissolved CO_2 per 1000 years. For this higher advection rate, dissolved CO_2 comprises less than 14 % of the total CO_2 in the overburden, much less than for the near-hydrostatic scenario. This is because a greater part of the overburden section is swept by the free CO_2 plume within which the concentration fraction of dissolved CO_2 is limited at 0.05, the saturation limit, some 7% by weight of free CO_2.

4. Analysis of Sleipner time-lapse seismic data

It is instructive to assess whether the time-lapse monitoring data are compatible with overburden behaviour showing these putative very low migration rates.

The CO_2 plume at Sleipner does lie beneath a number of seismic bright-spots indicative of earlier natural gas (largely methane) migration and accumulation in the vicinity (Fig. 8). One bright-spot (A) lies just above the Utsira Sand and another (B) lies in a shallower layer which holds a number of other bright-spots. This ‘gassy layer’ is widespread in the Sleipner area and is interpreted as holding significant naturally-occurring gas in the pore-space. Both bright-spots are underlain by vertical zones of more chaotic and attenuated reflections interpreted as small chimneys (note that features A_m and B_m are artefacts arising from multiple reflections from the seabed).

The distribution of bright-spots in the ‘gassy layer’ is mapped for the baseline survey in 1994 and also for a repeat survey in 2008 (Figs. 9a, b). The high amplitude patches mark individual bright-spots corresponding to discrete gas accumulations within the layer, with bright-spot (B) (Fig. 8) highlighted. Difference data (Fig. 9c) indicate relatively small time-lapse changes which can largely be ascribed to the various acquisition mismatches between the baseline and repeat surveys. Note that layers such as this, with strong and complex lateral changes in seismic velocity, are particularly susceptible to changes in acquisition geometry in terms of producing time-lapse differences. The greatest difference signal lies generally in the central and northern part of the mapped area and is largely outside the spatial footprint of the topmost CO_2 layer.

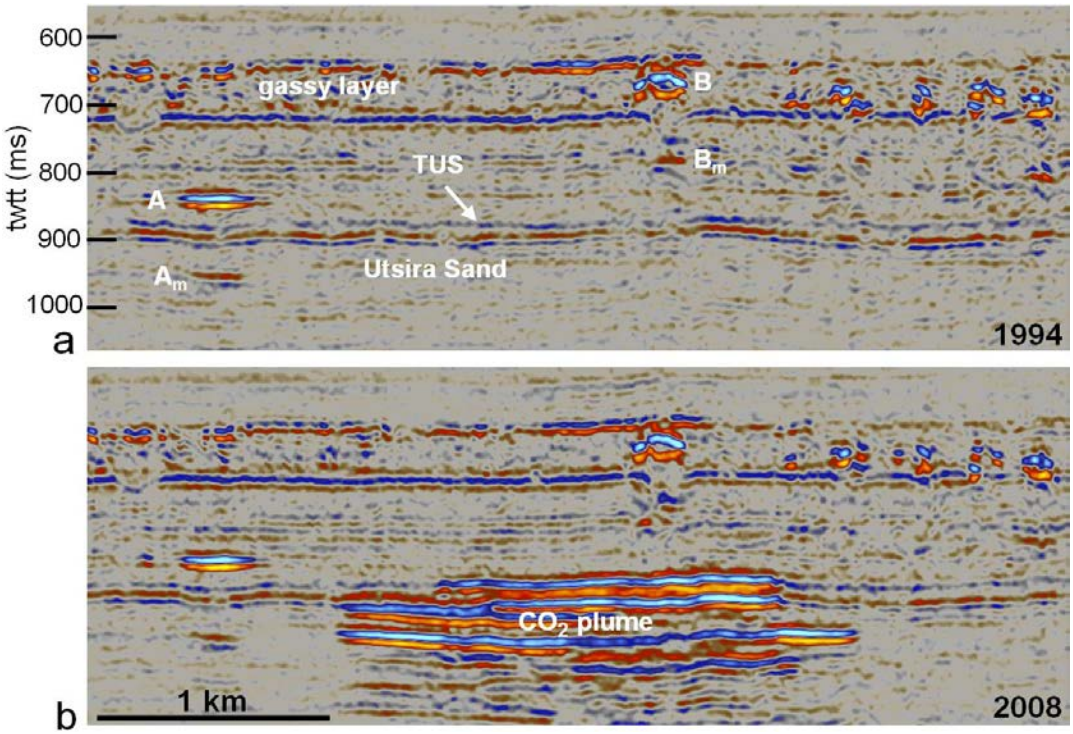

Fig. 8 Seismic features in the overburden at Sleipner. a) South-north section from the 1994 baseline dataset showing a minor overburden bright-spot (A) just above the Utsira Sand with a shallower bright-spot (B) lying within a more generally 'gassy' layer. b) Same section from the 2008 survey showing the same bright-spots and the highly reflective CO_2 plume within the Utsira Sand. Note feature B lies above a small 'feeder' chimney above the CO_2 plume. TUS = Top Utsira Sand; A_m and B_m are seabed peg-leg multiples (artefacts) from the overlying bright-spots.

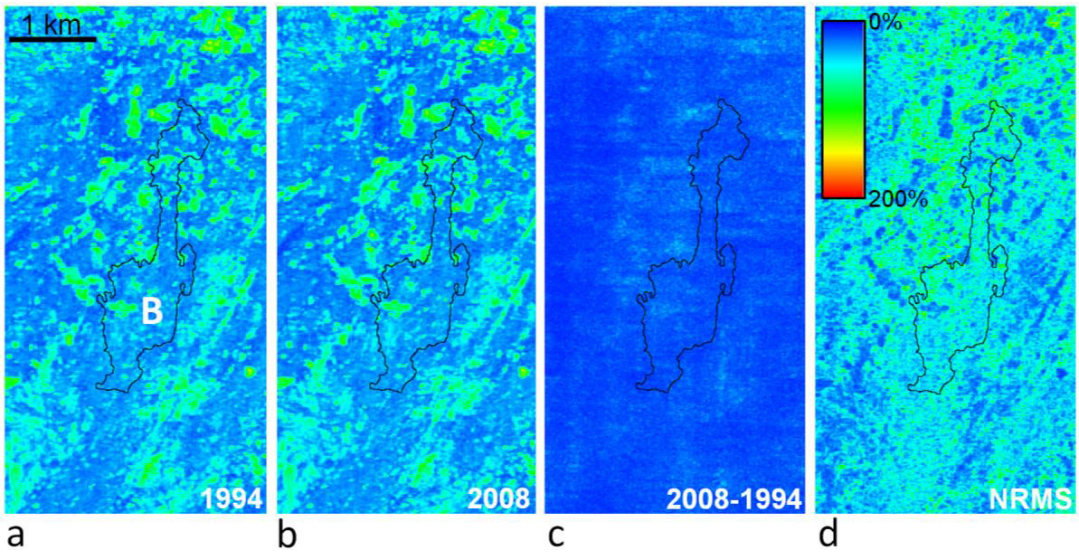

Fig. 9 Seismic amplitude attributes calculated for a 110 ms window centred on the gassy layer. a) RMS amplitudes in 1994 with bright-spot (B) indicated b) RMS amplitudes in 2008 c) RMS amplitude changes 2008 – 1994 d) NRMS 2008 to 1994. Yellow colours denote high amplitude values, blue colours low amplitude values. Black polygon denotes the lateral extent of the topmost layer of CO_2 in 2008.

A quantitative measure of time-lapse changes is the normalised RMS difference NRMS [19]. This is defined as the difference between two traces (a_t and b_t) in a specified time window divided by the average RMS amplitude of the two input traces:

$$NRMS = \frac{200 \times RMS(a_t - b_t)}{RMS(a_t) + RMS(b_t)} \quad (1)$$

where the RMS summation is over time window t.

For perfectly matched traces, with no repeatability error, NRMS is equal to zero.

NRMS mapping for the 'gassy layer' (Fig. 9d) shows low values (<20%), indicative of high repeatability, for the bright-spots, but with lower repeatability elsewhere where reflection strengths are much lower. Neither the difference nor the NRMS data (Figs. 9c, d) show any evidence of increased signal above the plume (if anything values are smaller above the plume) and there so is no indication of fluid saturation changes in the 'gassy layer' between 1994 and 2008.

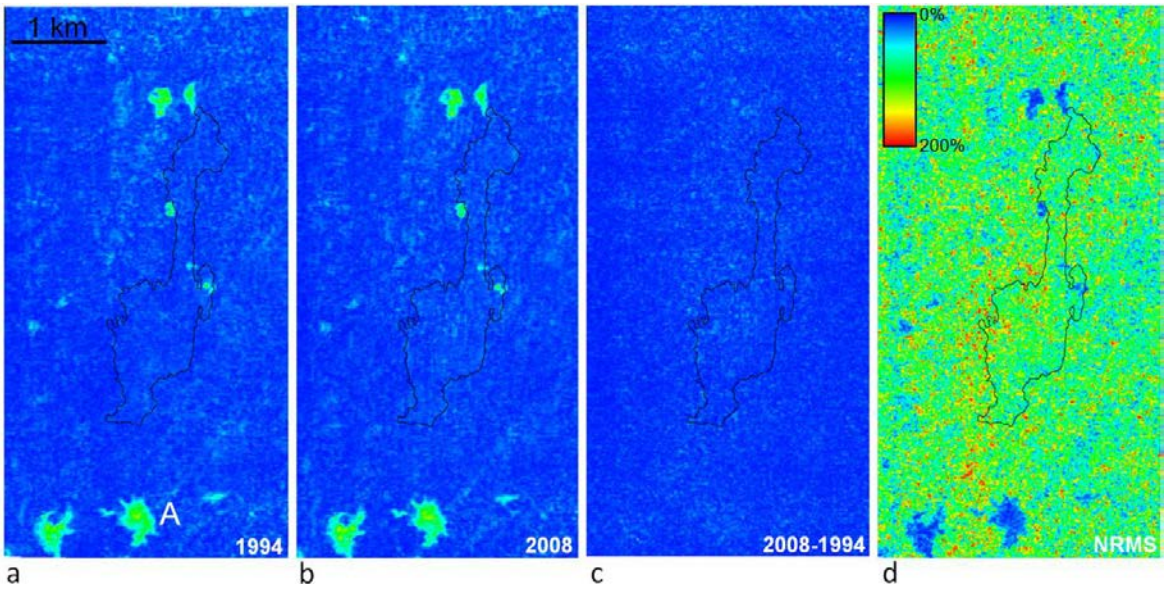

Fig. 10 Seismic amplitude attributes calculated for a 20 ms window centred 30 ms above the top Utsira Sand. a) RMS amplitudes in 1994 with bright-spot (A) indicated b) RMS amplitudes in 2008 c) RMS amplitude changes 2008 – 1994 d) NRMS 2008 to 1994. Yellow colours denote high amplitude values, blue colours low amplitude values. Black polygon denotes lateral extents of the topmost layer of CO_2.

Looking deeper, evidence for the possible egress of CO_2 into the overburden immediately above the topmost CO_2 layer in the reservoir can be assessed from time-lapse changes. Any change in fluid content in the overburden would induce time-shifts, signal attenuation and possible new bright-spots, all of which would be expected to increase NRMS values. A 20 ms window centred 30 ms above the top of the Utsira Sand was chosen for the analysis (Fig. 10). For time-lapse comparisons it is not practical to choose a window much closer to the top of the reservoir because side-lobe precursor energy from the near zero-phase wavelet of the topmost CO_2 reflection, and time-shifts associated with tuning effects (Furre et al. 2015), both result in significant reflection energy immediately above the stratigraphical top of the reservoir.

The distribution of bright-spots in the analysis window is mapped for the baseline survey in 1994 and also for the repeat survey in 2008 (Figs. 10a, b). The high amplitude patches mark individual bright-spots which correspond to discrete gas accumulations within the layer. The larger bright-spots all lie outside the footprint of the topmost CO_2 layer, with bright-spot (A) (Fig. 8) highlighted. Difference data (Fig. 10c) indicate relatively small time-lapse changes which, as above, are ascribed to the various acquisition mismatches between the baseline and repeat surveys. The greatest difference signal lies in the central and northern part of the mapped area and is largely outside the spatial footprint of the topmost CO_2 layer, with no systematic change of difference signal above the layer or, specifically, in the vicinity of the chimney beneath bright-spot B.

NRMS mapping for the analysis window (Fig. 10d) shows low values (<10%), indicative of high repeatability, for the bright-spots, but with significantly lower repeatability for the generally weakly-reflective overburden sequence elsewhere. As with the difference data, the NRMS data show no evidence of systematically increased signal above the topmost CO_2 layer, with no indication of fluid saturation changes in the overburden between 1994 and 2008.

In summary therefore, the time-lapse 3D seismics show no evidence of changes in the overburden above the plume, which includes a small chimney directly overlying the topmost CO_2 layer. Nor is there evidence of any change in the shallower 'gassy layer' higher in the overburden.

5. Discussion

By assuming some simple end-members for chimney properties we have placed lower limits on possible CO_2 migration rates in chimney-like overburden features. For the North Sea we have hypothesised that the observed chimneys are largely dormant features with gas present only in low saturations as a residual phase. Providing fracture dilation/shear pressures are not reached, then the bulk flow 'Darcy' properties of the strata, as measured in the laboratory, should be in line with these lower limits. In reality it is likely that, even below fracture pressure, fluid transport through these types of rocks is via some form of heterogeneous pathway flow of which the bulk property represents an average. In this respect, whereas overall flow fluxes (mass transport rates) are likely to be similar to the bulk modelling, localised breakthrough of the heterogeneous migration front to shallower depths is likely to be quicker than in the models.

Modelled flux rates of free and dissolved CO_2 range from 60 tonnes to 500 tonnes per thousand years. For a notional 100 Mt storage site these rates are several orders of magnitude below the maximum leakage threshold of ~0.01% per year which has been suggested as ensuring effective mitigation performance [20].

In addition, aside from dissolution, our numerical model does not incorporate geochemical processes. A number of studies [21, 22] indicate that the migration of CO_2 through typical argillaceous overburden lithologies would be significantly retarded and attenuated due to its reacting with the pore fluid to form new mineral phases.

An important point is that unlike advection, diffusive transport of CO_2 from the reservoir will not be restricted to chimneys or other potential pathway features, but will occur from the entire topseal contact footprint of the trapped CO_2 in a reservoir. Depending on the size of this footprint, diffusion might well be the dominant process by which CO_2 escapes from the reservoir.

Regarding the seismic monitoring, we have used difference amplitudes and NRMS to evaluate time-lapse changes. A more sensitive or forensic approach might be to look at very small time-shifts beneath the small chimney features which would be diagnostic of fluid saturation changes within the chimneys. This approach however is complicated by tuning-related time-shifts associated with thickening of the topmost CO_2 layer itself [23], and would require a sophisticated model-based statistical analysis.

6. Conclusions

Chimney-like overburden features might well comprise the principal geological containment risk for North Sea storage and also other settings where post-rift stratigraphical successions form the overburden. Using a simple numerical model we have placed a lower bound on potential out-of-reservoir-migration based on advective and

diffusive transfer through dormant overburden chimney features where the capillary seal has been removed, but which otherwise have similar properties to intact overburden. This is applicable to storage situations where reservoir pressures do not reach the fracture dilation or shear threshold. Modelled migration rates of the CO_2 range between 0.02 m and 0.2 m per thousand years depending on the amount of overpressure in the storage reservoir (near-hydrostatic and approaching fracture pressure respectively). These figures assume Darcy advective flow and diffusion based on effective bulk rock properties, so any heterogeneous pathway flow would likely lead to localised instances of more rapid fluid transit, but not to larger fluxes overall. For a 100 Mt storage site modelled flux rates of free and dissolved CO_2 are several orders of magnitude below the leakage thresholds required to ensure effective mitigation performance. Time-lapse 3D seismic reflection data show no evidence of changes in the overburden above the CO_2 plume and so are consistent with the dormant chimney model.

Acknowledgements

This paper is published with permission of the Executive Director, British Geological Survey (NERC). The Sleipner licence partners are acknowledged for releasing the seismic data presented in this paper.

References

[1] Cartwright J, Huuse M, Aplin A. Seal bypass systems. Am. Assoc. Pet. Geol. Bull. 2007; 91:1141-1166.
[2] Løseth H, Wensaas L, Arntsen B, Hanken N-M, Basire C, Graue K. 1000m long gas blow-out pipes. Marine Geology 2011; 28:1047-1060.
[3] Karstens J, Berndt C. Seismic chimneys in the Southern Viking Graben – Implications for palaeo fluid migration and overpressure evolution. Earth & Planetary Science Letters 2015;412: 88-100.
[4] Siegert MJ, Dowdeswell JA, Hald M, Svendsen J-I. Modelling the Eurasian Ice Sheet through a full (Weichselian) glacial cycle. Glob. Planet. Change 2001;31:367-385.
[5] Kleman J, Fastook J, Ebert K, Nilsson J, Caballero R. Pre-LGM Northern Hemisphere ice sheet topography. Clim. Past 2013;9:2365-2378.
[6] Baklid A, Korbøl R, Owren G. Sleipner Vest CO_2 disposal, CO_2 injection into a shallow underground aquifer. SPE paper 36600, presented at 1996 SPE Annual Technical Conference and Exhibition, Denver Colorado, USA. 1996.
[7] Chadwick RA, Holloway S, Kirby GA, Gregersen U, Johannessen PN. The Utsira Sand, Central North Sea – an assessment of its potential for regional CO_2 disposal. In: Williams D, Durie I, McMullan P, Paulson C, Smith A, editors. Greenhouse Gas Control Technologies. Proceedings of the 5th International Conference on Greenhouse Gas Control Technologies. CSIRO Publishing; 2001; p. 349 – 354.
[8] Zweigel P, Arts R, Lothe AE, Lindeberg ERG. Reservoir geology of the Utsira Formation at the first industrial-scale underground CO_2 storage site (Sleipner area, North Sea). In: Baines S, Gale J, Worden RJ, editors. Geological Storage for CO_2 Emissions Reduction. Special Publication 233 of the Geological Society, London; 2004. p. 165–180.
[9] Arts RJ, Chadwick RA, Eiken O, Dortland S, Trani M, Van Der Meer LGH. Acoustic and elastic modelling of seismic time-lapse data from the Sleipner CO_2 storage operation. In: Grobe M, Pashin J, Dodge R, editors. Carbon Dioxide Sequestration in Geological Media – State of the science. AAPG Studies in Geology; 2010; 59:391 – 403.
[10] Chadwick RA, Williams GA, Williams JDO, Noy DJ. Measuring pressure performance of a large saline aquifer during industrial scale CO_2 injection: the Utsira Sand, Norwegian North Sea. International Journal of Greenhouse Gas Control 2012; 10: 374-388.
[11] Harrington JF, Noy DJ, Horseman ST, Birchall DJ, Chadwick RA. Laboratory study of gas and water flow in the Nordland Shale, Sleipner, North Sea. In: Grobe M, Pashin J, Dodge R, editors. Carbon Dioxide Sequestration in Geological Media – State of the science. AAPG Studies in Geology; 2009; 59:521-543.
[12] Springer N, Lindgreen H. Cap rock properties of the Nordland Shale recovered from the 15/9-A11 well, the Sleipner area: Proceedings of the 8th International Conference on Greenhouse Gas Control Technologies, Trondheim, Norway, June 19-22, 2006: Oxford, Elsevier, CD-ROM.
[13] Pruess K. ECO2N: A TOUGH2 Fluid Property Module for Mixtures of Water, NaCl, and CO_2. Lawrence Berkeley National Laboratory Report LBNL-57952. 2005.
[14] Pruess K, Oldenburg C, Moridis G. TOUGH2 User Guide, version 2.0. Lawrence Berkeley National Laboratory Report LBNL-43134. 1999.
[15] Alnes H, Eiken O, Nooner S, Sasagawa G, Stenvold T, Zumberge M. Results from Sleipner gravity monitoring: updated density and temperature distribution of the CO2 plume. Energy Procedia 2011;4:5504-5511.
[16] Chadwick RA, Noy DJ. Underground CO_2 storage: demonstrating regulatory conformance by convergence of history-matched modelled and observed CO_2 plume behavior using Sleipner time-lapse seismics. Greenhouse Gases: Science & Technology 2015; 5:305-322. 10.1002/ghg.
[17] Chadwick RA, Arts R, Eiken O, Kirby, GA, Lindeberg E, Zweigel P. 4D seismic imaging of a CO_2 bubble at the Sleipner Field, central North Sea. In: Davies RJ, Cartwright JA, Stewart SA, Lappin M, Underhill JR, editors. 3D seismic technology: Application to the Exploration of Sedimentary Basins. Geological Society; 2004; p. 311–320.
[18] Evans D, editor. The Millenium Atlas: Petroleum Geology of the Central and Northern North Sea. Geological Society of London; 2003.
[19] Kragh E, Christie P. Seismic repeatability, normalized rms, and predictability, Leading Edge 2002; 21(7): 642-647.

[20] Hepple RP, Benson SM. Implications of surface seepage on the effectiveness of geological storage of carbon dioxide as a climate change mitigation option. In: Gale J, Kaya Y, editors. Greenhouse Gas Control Technologies. Volume 1, Elsevier Science Ltd, Oxford, UK; 2003. p.261–266.

[21] Rochelle CA, Czernichowski-Lauriol I, Milodowski, AE. The impact of reactions on CO_2 storage in geological formations: a brief review. In: Baines S, Gale J, Worden RJ, editors. Geological Storage for CO_2 Emissions Reduction. Special Publication 233 of the Geological Society, London; 2004. p. 87-106.

[22] Balashov VN, Guthrie GD, Lopano CL, Hakala JA, Brantley SL. Reaction and diffusion at the reservoir/shale interface during CO_2 storage; Impact of geochemical kinetics. Applied Geochemistry 2015; 61:119-131.

[23] Furre AK, Kiær A, Eiken O. CO_2-induced seismic time shifts at Sleipner. Interpretation 2015; 3(3):23–35.